KSME

Springer

Journal of Mechanical Science and Technology 34 (8) 2020

Original Article
DOI 10.1007/s12206-020-0716-0

Keywords:
· Aeroengine
· Cylindrical roller bearing
· Skid damage
· Wear

Correspondence to:
Jun Luo
luojun_gyu@sina.com
Jin Xu
jinxu618@163.com

Citation:
Xie, X., Xu, J., Luo, J. (2020). Analysis of skid damage to cylindrical roller bearing of mainshaft of aeroengine. Journal of Mechanical Science and Technology 34 (8) (2020) 3239~3247.
http://doi.org/10.1007/s12206-020-0716-0

Received February 8th, 2020
Revised May 6th, 2020
Accepted May 19th, 2020

† Recommended by Editor Chongdu Cho

Analysis of skid damage to cylindrical roller bearing of mainshaft of aeroengine

Xiangyu Xie[1], Jin Xu[2] and Jun Luo[1]

[1]Guizhou Provincial College-based Engineering Research Center for Materials Protection of Wear and Corrosion, College of Chemistry and Materials Engineering, Guiyang University, Guiyang 550005, China, [2]School of Mechanical Engineering, Guizhou University, Guiyang 550025, China

Abstract Skid damage to mainshaft bearings on aeroengines severely reduces aircraft reliability. In this study, a batch of cylindrical roller bearings extracted from mainshaft of in-service aeroengines with, skid damage after a certain service period, were collected, and damage features of the bearings were characterized and compared with those of the undamaged bearings and the new ones. Microscopic feature evaluation, elemental analysis as well as the composition distribution of the bearings were conducted using scanning electron microscopy with energy-dispersive X-ray spectroscopy, X-ray diffractometry, X-ray photoelectron spectroscopy, transmission electron microscopy and surface profilometry. Analysis results reveal that skidding itself is a very complex process initiated by the action of different mechanisms, and manifest in different wear types. The damage mechanism of skid damaged bearings was the joint consequence of abrasive wear, oxidation wear and delamination wear. All the aforementioned damage and wear led to severe aircraft failures.

1. Introduction

Cylindrical roller bearings have been extensively widely used in the aircraft industry, which is ascribed to their exceptionally low-friction torque characteristics, making them the ideal part for high-speed operations [1]. Aeroengines bear the brunt of high speed, therefore, they must be highly durable and reliable. In addition, roller bearings that can function at the temperatures of over 200 °C and the speeds of more than 2.5 million *DN* (the product of shaft diameter in mm, and the rotating speed in r/min) are needed in aeroengines [2]. Such extreme working conditions result in the premature failure of cylindrical roller bearings in the mainshaft. In actual practice, damage to a rolling bearing is usually the joint consequence of several mechanisms operating. Notably, it is the complex combination of numerous influencing parameters, making it difficult to establish the primary cause of damage. As proved in the relevant literature and practical experience, bearings are the most critical elements governing the overall system performance [3].

Aeroengines have been developed towards the higher speed and higher thrust-weight ratio, and skid damage has been identified as the main influencing factor leading to premature failure in cylindrical roller bearings, which severely affects the service life and reliability of aeroengines. Therefore, skidding has always been a hot issue among the interested scholars, and a number of studies have been proposed for evaluating such failures [4-6]. To incur skid damage, slip must be present, but it is not given that damage will always occur in the presence of slip. Instead, many factors, such as wrong bearing alignment, light- or heavy-load application, improper lubrication, presence of foreign particles, bearing-material cleanliness, and other operating conditions, are responsible for skid damage to bearings. In other words, skid damage is a comprehensive failure that requires integrated research in multiple disciplines and fields. Recently, various studies have investigated the skidding behavior under ideal hypotheses or the given circumstances with theoretical models or experimental methods [7-10]. However, in these studies, the bearings are operated under ideal conditions selected by researchers, and

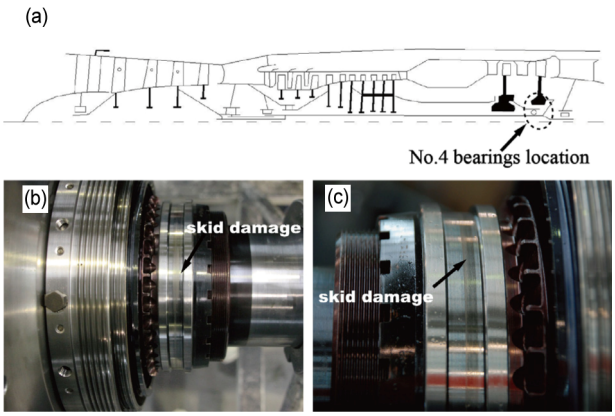

Fig. 1. Cylindrical roller bearing on mainshaft of aeroengine: (a) schematic diagram of installation position; (b) skid-damaged area; (c) alternate angle of skid damage shown in another roller bearing.

most results are different from those encountered in practical situations. Failure analysis is a tool which may be used by mechanical engineers and metallurgists to modify and increase the life and quality of machine components, failure cases [11-16] and numerical approaches [17-20] have been conducted to simulate damage phenomena. Although some studies [21, 22] on the characteristics of mainshaft bearings has been carried out, they mainly focus on the macroscopic properties and external appearance to determine whether there is skid damage to the bearings. Yet the damage characterizations behind skidding remain largely unclear, so the main damage mechanism should be further identified in a comprehensive study and extensive analysis. In this paper, a large number of skid damaged bearings were collected from the aeroengine maintenance shops to characterize the damage features and mechanisms of bearing skidding, with the main focus on characterizing the microstructural changes occurring on the bearing surface. In addition, the probable cause of such damage was briefly discussed, which might provide certain reference for improving the performance and service life of aeroengine bearings, as well as having practical value to the study regarding the reliability of roller bearings.

2. Test details

2.1 Parameters of bearings

The cylindrical roller bearings investigated in this study were the No.4 bearings installed on the mainshaft collected during the test run process and after flight of aeroengine, which was a variant of model WP-13 (Fig. 1(a)). The bearings were asssembled to the aeroengine that was subject to 2 hours of test run process or 300 total flight hours. As discovered after investigating twelve sets of the bearings, the typical failure observed was a consequence of skidding (Figs. 1(b) and (c)).

The characteristics of the roller bearings investigated are exhibited in Table 1. The inner rings and rollers were made of M50 (bearing steel, C = 0.75 %-0.85 %, Cr = 3.75 %-4.25 %, Mo = 4.00 %-4.50 %, V = 0.90 %-1.10 %, Ni $\leq$ 0.2 %, Mn $\leq$ 0.35 %, Si $\leq$ 0.35 %, and Fe to balance), and the cage components were made of silicon bronze with a silver coating. The bearing operating cofnditions are given in Table 2.

Table 1. Bearing structural parameters.

Bearing outside diameter (mm)	180
Bearing width (mm)	24
Pitch diameter dm (mm)	155
Number of rollers	30
Roller diameter dr (mm)	12
Roller length l (mm)	12
Free diametral clearance (μm)	60-120

Table 2. Operating conditions of cylindrical roller bearings of aeroengine mainshaft.

Lubricant	MIL-L-7808
Oil-flow rate (L/min)	3-13
Bearing temperature (°C)	170
Maximum speed (rpm)	12000
Maximum radial load (kN)	5
Run time (h)	2-300

2.2 Inspection techniques and equipment

The microscopic morphology and composition of the bearings were examined by focused-ion-beam scanning electron microscope (FIB-SEM, SCIOS, FEI) and energy-dispersive X-ray spectroscopy (EDS, Octane Pro) system. The phase composition of the bearing surface was analyzed by X-ray diffractometry (XRD, D/max 2500, Rigaku Corp.) at a glance angle of 3º. Meanwhile, the compositional and chemical states of the inner ring were analyzed through X-ray photoelectron spectroscopy (XPS, PH Quantera II, Ulvac-Phi). The structure and morphology were determined by tansmission electron microscopy (TEM, Tecnai G2 20, FEI) operating at 200 kV. A stylus profilometer (Talysurf Stylus PGI420, Taylor Hobson) was employed to obtain the profiles of the inner rings and rollers. In addition, the cross-sections of both the inner rings and rollers (using a 4 % solution of nitric acid in alcohol) were etched to gather information via an optical microscope (OM, Axio Vert.A1, Zeiss).

3. Results and discussion

3.1 Damage characterization of inner ring

The actuating bearing was disassembled for inspection and investigation. As a result, the worn surface direction of the inner ring was coincided with the bearing rotational direction (Fig. 2(a)). This worn area had a circular shape with no any connections, implying that the inner ring bore an uneven weight and centrifugal load. Meanwhile, the raceway color in the skid

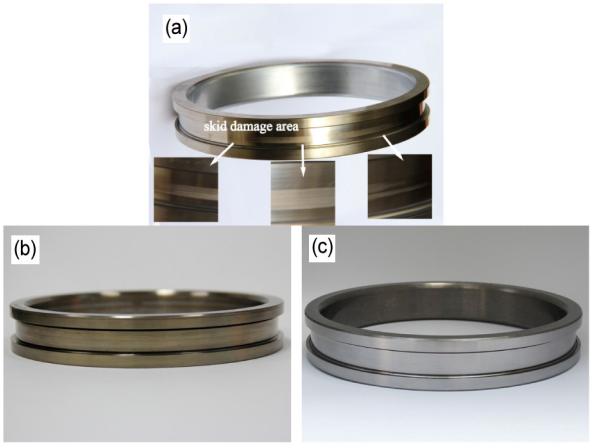

Fig. 2. Surface of inner ring (a) with and (b) without damage; (c) shows a new inner ring.

damaged inner ring and the undamaged inner ring turned brown (Fig. 2(b)) when compared with that of the new one, which was characterized as discoloration possibly induced by oil decomposition (Fig. 2(c)), thus reflecting the complex lubrication of the bearing when in mainshaft service.

As is evident from the images provided of the skid damaged inner ring (Fig. 3(a)), the inner ring surface was covered in multiple pits. Moreover, the pits shapes differed in appearance and showed no connect with one another. Notably, the micro-pits revealed the occurrence of local metal-to-metal contact. Furthermore, the micro-pits also showed that a small fraction of material had spalled from the inner ring surface, resulting in ploughing at the rotational direction. With regard to the undamaged inner ring, there were long scratches at the rotational direction, with holes presented on the surface (Fig. 3(b)). As for the new inner ring, only pits were observed, which might result from the lapping processing (Fig. 3(c)). In line with the wear theory [23], abrasion is the plastic deformation or separation of material from the contacting surfaces due to a relative motion, micro-plowing, micro-chipping, micro-fatigue, and micro-fractures may occur. It can be concluded that abrasive wear accounts for the primary cause of skid damage from the above features.

The XPS spectrum of Fe 2p for the skid damaged and new inner ring are shown in Fig. 4. The binding energies of Fe $2p_{3/2}$ obtained from the new inner ring were 708.1 eV and 706.8 eV, respectively (Fig. 4(b)), which lied between the values obtained for Fe_3C and Fe. For the skid damaged area in inner ring, an extra peak (709.5 eV) was observed in the XPS spectrum obtained for FeO (Fig. 4(a)). Such discrepancy might be attributed to the oxidation on surface, and the presence of this peak and the binding energy were consistent with those reported by other researchers [24], demonstrating the occurrence of oxidation wear during the skidding process.

Further, FIB-SEM was applied to examine some selected areas from the skid damaged inner ring to acquire more information. After the pitted areas were thinned through sputtering, the pits depth was ascertained to be 1-4 μm (Fig. 5). Moreover, transverse cracks were present at the bottom of the pits. It was

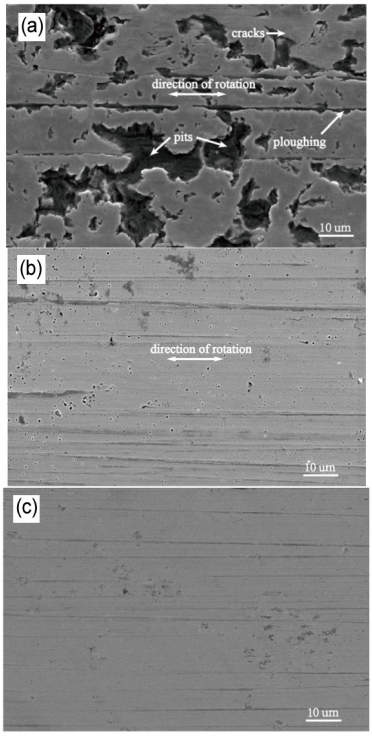

Fig. 3. Microscopic features of the inner ring surface (a) with and (b) without damage; (c) shows a new inner ring.

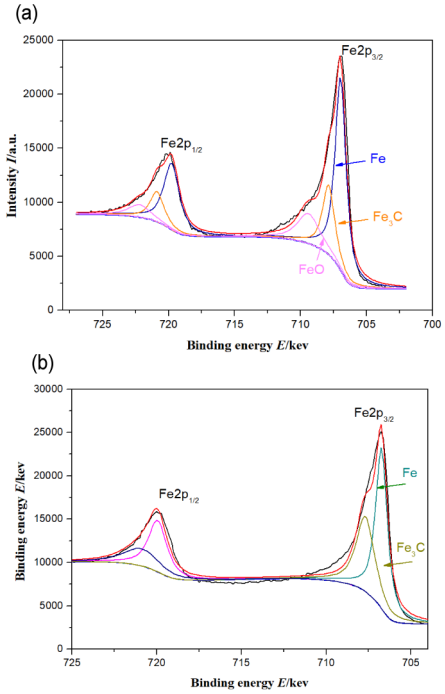

Fig. 4. The XPS spectrum: (a) skid damaged; (b) new inner ring.

observed that some micro-cracks on the surface of the inner ring had penetrated the pits (Fig. 6(a)). Actually, a longitudinal crack approximately 2.5 μm depth was observed after milling, the angle of which was 75° (Fig. 6(b)).

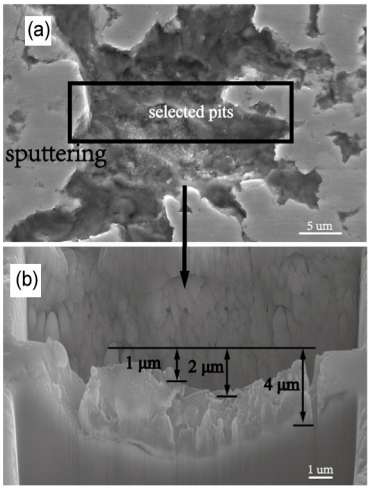

Fig. 5. Sputtering thinning of pitted areas using FIB: (a) selected pits; (b) measurement of pit depths.

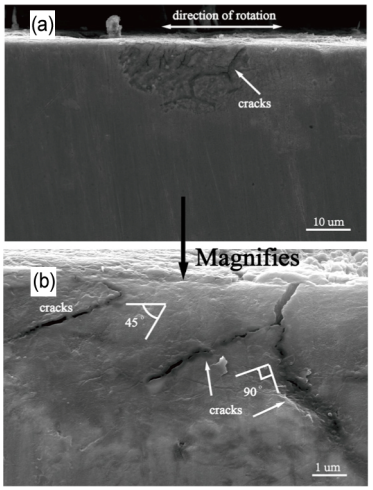

Fig. 7. Cross-section of skid damaged inner ring.

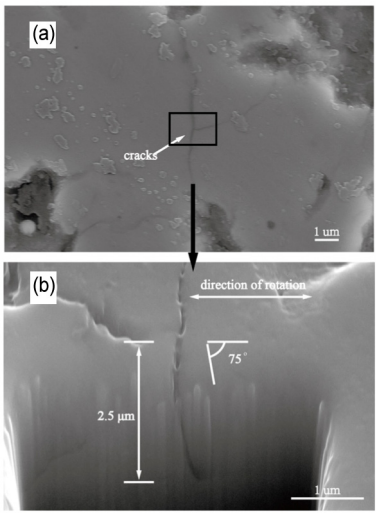

Fig. 6. Skid damaged inner ring: (a) micro-cracks penetrating the pits; (b) a longitudinal crack.

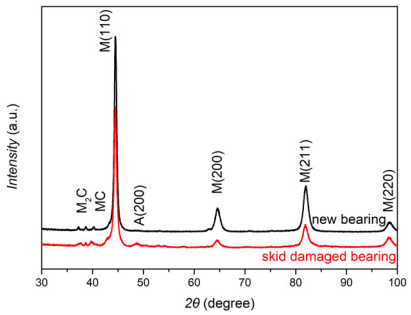

Fig. 8. XRD patterns of skid-damaged and new inner rings.

Moreover, the cross-section of the skid damaged inner ring was also observed. The cracks were attributed to surface contact, which were approximately 2-10 μm in width and approximately 20 μm in length (Fig. 7). The cracks were oriented at an angle approximately 45° to the contact surface at the rotational direction. Meanwhile, the longitudinal crack was perpendicular to the extended one, which implied the continuously worsening situation. Such cracks initiated as the small scratches at the beginning, but they grew larger through summation. Noteworthily, the maximum von Mises stress during rolling contact also occurs at a similar depth [25]. The results of microscopic investigation suggested that delamination wear occurred during skidding of the inner raceway. Therefore, it was reasonably assumed that, these cracks resulted from the strains developed on the sub-surface during rolling contact. Besides, the cracks further propagated to the surface and finally lead to bearing spalling. According to the results [26], for the friction pair made of quenched and tempered steel, cracks initiate on the surface, then propagate to the sub-surface along the rolling direction, and finally become the fan-shaped fatigue pit, which is ascribed to the combination of rolling and sliding motions on surfaces. Moreover, subsurface crack initiate on the subsurface, then expand to both sides parallel to the surface, and finally fracture at both sides to form a shallow pit on the specimen width. Presently, skid damage in aircraft manufacturing and repair plants is controlled by grinding the surface of the inner ring raceway [27]; however, the purpose of grinding the surface of inner ring raceway is not to prevent skid damage.

The XRD pattern of surface with new and skid damaged inner ring are shown in Fig. 8. For the inner ring sample, a mixture of austenite and martensite was found, which was consistent with relevant literature [28]. Nonetheless, the peaks of austenite (200) were observed on the skid damaged surface, indicating austenization, and some carbon were dissolved in martensite matrix during this process, resulting in a decrease of martensite. Surface material transfer occurred simultaneously, therefore, chemical composition changed during the skidding process. The grain size of the top surface of skid damaged inner ring was smaller than that of the matrix structure, and the morphologies of martensite and austenite changed significantly

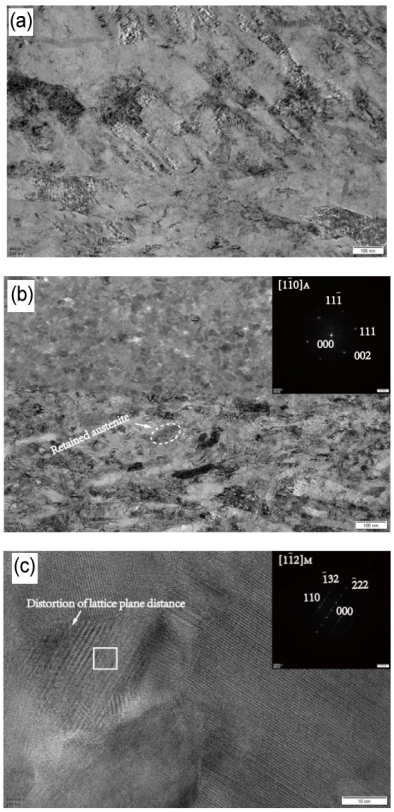

Fig. 9. TEM images of (a) matrix structure; (b) top surface of skid damaged inner ring; (c) HRTEM images of (b).

(Fig. 9(a)). In terms of the top surface of the skid damaged inner ring, part of the original martensite lath disappeared, which formed smaller micro-laths, micro-crystals and micro-twin crystals. In the meantime, the retained austenite phase was dispersed on the martensite (Fig. 9(b)). The substructure of martensite was studied by HRTEM, which revealed the distortion of the lattice-plane distance (Fig. 9(c)). Based on the TEM diffraction patterns of the [110] and [112] zone axis and the Fe-C phase diagram [29, 30], it was inferred that the phase in Fig. 9(b) was ɣ-Fe formed after skidding, which confirmed that the surface temperature reached the phase transition, causing austenization under the action of high temperature.

3.2 Damage characterization of the rollers

Macroscopic examination showed that, the most prominent features of skid damage on the rollers were bands of oil film, discoloration (a dark brown oxide film), and circular deposition adhesion of the rollers (Fig. 10(a)). In the undamaged roller (Fig. 10(b)), color of the area was darker than that in the new roller (Fig. 10(c)).

Besides, the damage on the roller surface was significant (Fig. 11). For instance, there were multiple holes across the entire roller surface, along with evident ploughing at the rotational direction of the roller (Fig. 11(a)). The roller might be subject to two-body and three-body wear, and intense plastic

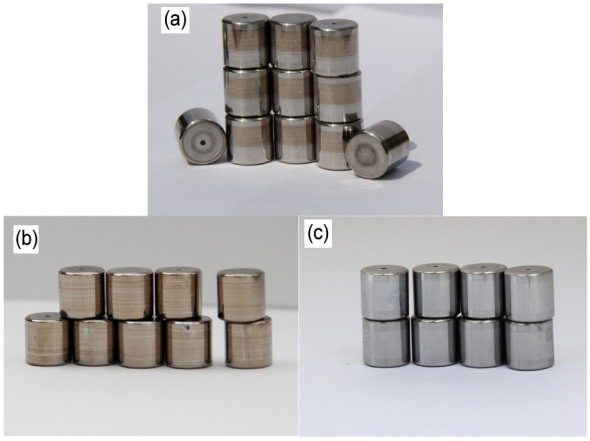

Fig. 10. Rollers (a) with and (b) without damage; (c) shows a new roller.

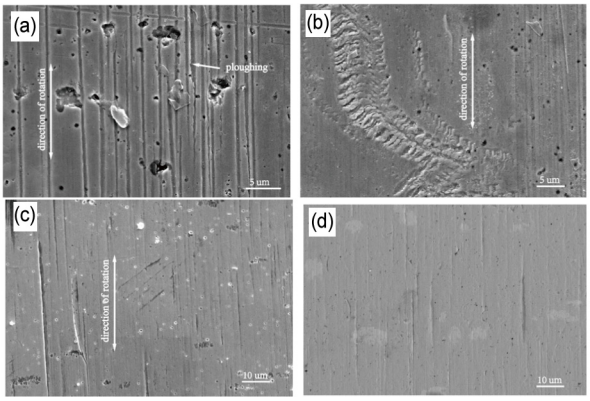

Fig. 11. Roller surface: (a) holes and ploughing; (b) plastic deformation in skid-damaged roller; (c) undamaged roller; (d) new roller.

deformations (with irregular shapes) were also seen (Fig. 11(b)), which might occur due to the local high stress on the convex position of the rough surface when the friction components moved relative to each other [31]. Microscopic observation in both the undamaged and new rollers show less abnormal features, holes, and scratches in the direction of rotation presented on the undamaged roller surface (Fig. 11(c)), which seemed to be inevitable during the high-speed operation process. Some scratches in the new roller indicated that its machining precision was insufficient (Fig. 11(d)). In addition, it was shown that, the roller suffered from abrasive wear in the process of skid damage, and the cause of the roller abrasion was consistent with that of the cause of raceway abrasion.

Furthermore, the surfaces of the rollers were examined by EDS (Fig. 12). As a result, for the skid damaged roller, there was excess elemental O (compared with a new roller), implying that the roller experienced oxidation wear. In line with theory [32], plastic deformation may accelerate the diffusion of O into the metal, and a new film will be formed after the oxide film has fallen off. Consequently, high temperature and the impact speed of the inner ring may aggravate oxidation wear, but decrease the extent of oxidation of the roller.

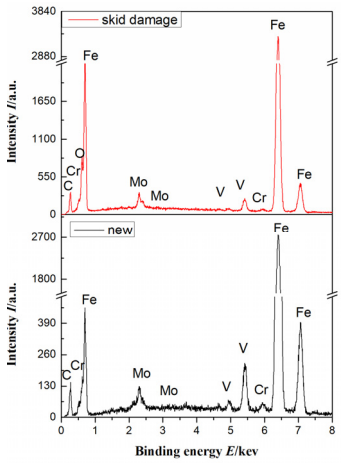

Fig. 12. EDS results of new roller and skid damaged roller.

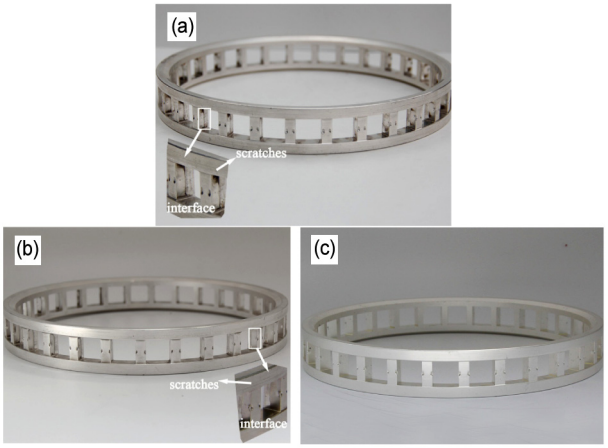

Fig. 13. Macroscopic image of cage: (a) skid damaged; (b) undamaged; (c) new cage.

3.3 Damage characterization of the cages

According to the macroscopic examination (on both skid damage and undamaged cage), a scar occurred at the interface between the cage and roller, while a new cage was shiny and in good condition (Fig. 13). Severe wear was revealed from the low magnification inspection of the cage interface (Fig. 14(a)), including scratches and multiple holes on the cage surface (Fig. 14(b)), as well as several dark objects embedded in the surface (Fig. 14(c)). Furthermore, the dark objects were examined with EDS, and the results showed the presence of elemental Fe (Fig. 14(d)). The cage was coated with silver, which provided it with strong corrosion resistance and improved the running properties of the harder bearing materials, but the silver coating and cage material were relatively soft. The lubrication system of the aero-engine mainshaft was filtered via a coarse filter with an average pore diameter of 72 μm, but the oil quality and lubricant status were operating properly. It was predicted that, the dominance of abrasion in a cage under lubrication might be due to the existence of metal particles or material spalling from the raceway and roller of mainshaft bearings.

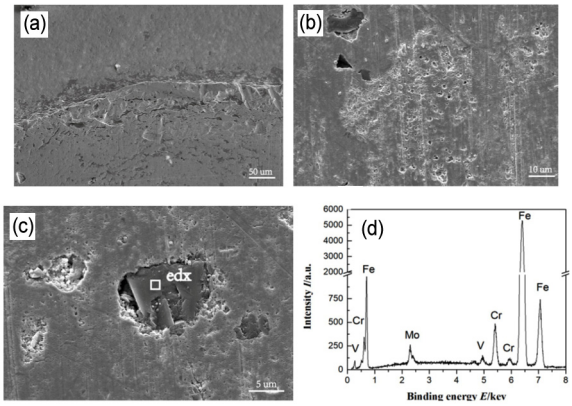

Fig. 14. Skid damaged cage interface: (a) low magnification; (b) multiple holes; (c) several dark objects embedded in surface; (d) edx result of the selected zone of skid damaged cage.

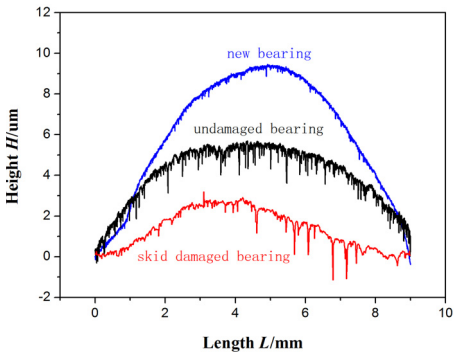

Fig. 15. Profile of inner ring.

3.4 Microscopic profile and structure between inner ring raceway and roller surface

It can be seen that the new inner ring had a smoother profile than that of the skid damaged and the undamaged inner ring (Fig. 15). Compared with the new inner ring, the undamaged inner ring experienced significant dimensional reduction. The profile of the skid damaged inner ring turned linear, and which was 8 μm and 3 μm lower than that of the new inner ring and the undamaged one, respectively. Generally, ideal lubrication of a cylindrical roller bearing occurs when an oil film completely separates the rollers from the inner ring, so that there is no metal to metal contact between the roller and the inner ring. Such phenomenon shows that, there is wear during the bearing operation process, and skid damage occurs owing to the worsened working condition.

Rollers had significantly different shapes (Fig. 16). For instance, the profile of skid damaged rollers was irregular, and had a maximum height dimension of approximately 2 μm, whereas the new roller and the undamaged one were smooth in height. It was observed that, the partially crowned profile of the new roller was more regular than those of the skid damaged and the undamaged rollers. Further visual examinations revealed that, the oil film bands on the roller had reduced diameter. It was concluded based on the FEM solutions [33], it

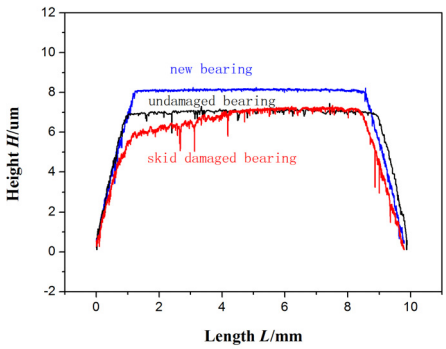

Fig. 16. Surface profiles of skid damaged, undamaged and new rollers.

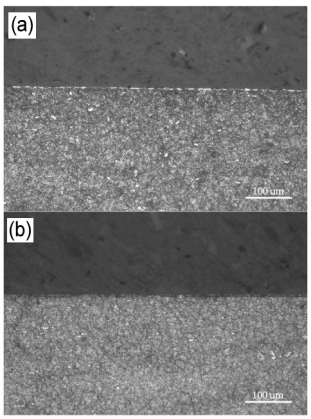

Fig. 17. Metallographic structure of (a) skid damage; (b) undamaged inner ring.

can be concluded that partially crowned profiles of both the new and undamaged roller tend to generate less edge stress under a given load as compared with the skid damaged profile. Rolling elements were exposed to complicated loadings during the flights, for this type of bearing, radial load was in the range of 0 to 5 kilonewton during the flights. Static loadings act on the rolling elements at the steady-state conditions. However, dynamic loadings are more prominent since the conditions are changeable while flying. Each part especially for roller responds dynamically to the forces acting. Moreover, the roller exhibits more intense response in the extreme conditions such as zero load presented and result in bearing slip, then skid damage might took place.

The metallographic structure of the inner ring features was characterized by residual austenite, martensite and carbide. Moreover, thin and discontinuous white bands occurred along the skid damaged inner ring boundary (Fig. 17(a)), but no abnormal structures was found in the undamaged inner ring (Fig. 17(b)). On the other hand, metallographic examination suggested that, the undamaged roller (Fig. 18) contained martensite, residual austenite and carbide, which were evident in the of the roller cross-sections after etching. In the skid damaged roller (Fig. 19), the volume percentage of residual austenite was less than that of the undamaged roller. Further, the continuous white bands were observed along the roller boundary

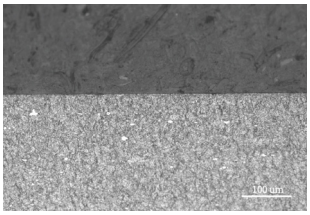

Fig. 18. Metallographic structure of undamaged roller performed on transverse sections.

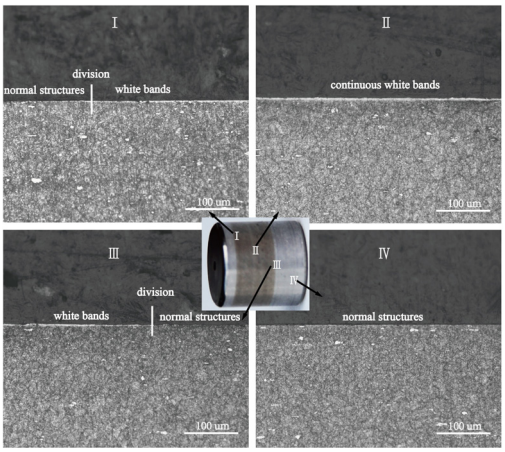

Fig. 19. Metallographic structure of the skid damaged roller.

in parts of the oil film. When moved to the boundary of the oil film, it was evident that the white bands and normal structures of the roller dominated different positions (performed on the transverse sections). The wear volume corresponds to the length of macroscopic oil film bands, which suggested a trend of progressive material loss. When a bearing undergoes repeated rolling and sliding contacts under high temperature and elasto-hydrodynamic lubricated conditions, the microplastic deformations will accumulate, which manifests as the white etched bands [34]. Therefore, combined with the damage characterization, XRD, XPS and TEM results, one can postulate the reasons for certain observations, for instance, the white bands are formed as a result of the plastic deformation mechanism during rolling contact, and the metal to metal contacts of the inner ring and roller increase the temperature to the austenitic temperature. The white bands on the inner ring became discontinuous, which was possibly because of presented features in the pitted area.

The mechanism for the skid damage in mainshaft bearings of aeroengines is quite complicated, and it is suggested that the skid damage process initiated by the action of different wear mechanisms such as abrasive wear and delamination wear. As stated previously, crowning of rollers and raceways is accomplished to avoid edge loading that can result in failure of the rolling components. However, the current roller profile design is still insufficient due to the characteristics after skid damage. In this regard, a “logarithmic” profile is recommended [35], and it is named because it can be expressed mathematically as a special logarithmic function for yielding a substantially

optimized stress distribution. Under misalignment and most other conditions, edge loading tends to be avoided relative to the current partially crowned roller profiles. Additionally, the problem source of abrasion in the cage is found to be a coarse filter that accumulates the existence of metal particles embedded into the cage surface, and the use of a lower grid filter may eliminate the possibility of contamination in lubrication system. It is believed that, the full-scale tests under controlled conditions can best estimate the working state of mainshaft bearings. In addition, the engine vibration, temperature and content of the lubricant during the tests should be closely monitored to determine the working state of the bearing. Certain limitations should be noted in this paper, namely, the unconventionality of bearings should be reproduced in test under typical engine conditions.

4. Conclusions

In the case of skid damage on the mainshaft bearings of aeroengines, the inner ring and rollers suffer from more severe damage in terms of both metallographic structure and surface profile dimension. The formation of white bands in the skid damaged inner ring and roller is the result of the plastic deformation during rolling contact, and the metal to metal contacts of the inner ring and roller increase the temperature to the austenitic temperature. The damage mechanisms of skid damage to cylindrical roller bearings on the mainshaft bearings of aeroengines may be the joint consequence of abrasive wear, oxidation wear and delamination wear.

Acknowledgments

This work was supported by the National Natural Science Foundation of China (Grant No. 51605105), Guizhou Excellent Youth Scientific and Technological Talent Program of China (Grant No. [2017]5628), Major Science and Technology Project in Guizhou Province (Grant No. Q.K.H.Z.D.Z.X.Z [2019]3016), Discipline and Master's Site Construction Project of Guiyang University by Guiyang City Financial Support Guiyang University (HC-2020).

References

[1] W. Tu, Y. Shao and C. Mechefske, An analytical model to investigate skidding in rolling element bearings during acceleration, *Journal of Mechanical Science and Technology*, 26 (2012) 2451-2458.

[2] G. Cavallaro, D. Nelias and F. Bon, Analysis of high-speed intershaft cylindrical roller bearing with flexible rings, *Tribology Transactions*, 48 (2005) 154-164.

[3] N. Ghaisas, C. Wassgren and F. Sadeghi, Cage instabilities in cylindrical roller bearing, *Journal of Tribology*, 126 (2004) 681-689.

[4] Y. Wang et al., Investigation of skidding in angular contact ball bearings under high speed, *Tribology International*, 92 (2015) 404-417.

[5] L. Oktaviana, V. Tong and S. Hong, Skidding analysis of angular contact ball bearing subjected to radial load and angular misalignment, *Journal of Mechanical Science and Technology*, 33 (2019) 837-845.

[6] Q. Han and F. Chu, Nonlinear dynamic model for skidding behavior of angular contact ball bearings, *Journal of Sound and Vibration*, 354 (2015) 219-235.

[7] S. Deng et al., Cage slip characteristics of a cylindrical roller bearing with a trilobe-raceway, *Chinese Journal of Aeronautics*, 31 (2018) 351-362.

[8] J. Li, W. Chen and Y. Xie, Experimental study on skid damage of cylindrical roller bearing considering thermal effect, *Proceedings of the Institution of Mechanical Engineers Part P-Journal of Sports Engineering and Technology*, 228 (2014) 1036-1046.

[9] A. Selvaraj and R. Marappan, Experimental analysis of factors influencing the cage slip in cylindrical roller bearing, *Int J Adv Manuf Technol*, 53 (2011) 635-644.

[10] T. Xu et al., A preload analytical method for ball bearings utilising bearing skidding criterion, *Tribology International*, 67 (2013) 44-50.

[11] S. Gürgen, M. Kuşhan and S. Diltemiz, Fatigue failure in aircraft structural components, *Handbook of Materials Failure Analysis with Case Studies from the Aerospace and Automotive Industries* (2016) 261-277.

[12] S. Gürgen, i. Saçkesen and M. Kuşhan, Fatigue and corrosion behavior of in-service AA7075 aircraft component after thermo-mechanical and retrogression and re-aging treatments, *Proceedings of the Institution of Mechanical Engineers, Part L: Journal of Materials: Design and Applications*, 233 (2018) 1764-1772.

[13] A. Toms and K. Cassidy, Filter debris analysis for aircraft engine and gearbox health management, *Journal of Failure Analysis and Prevention*, 8 (2008) 183-187.

[14] F. Cakir et al., Maintenance error detection procedure and a case study of failure analysis locomotive diesel engine bearings, *Journal of Failure Analysis and Prevention*, 18 (2018) 356-363.

[15] F. Çakir and O. Çelik, The effects of cryogenic treatment on the toughness and tribological behaviors of eutectoid steel, *Journal of Mechanical Science and Technology*, 31 (2017) 3233-3239.

[16] S. Diltemiz et al., Effect of dent geometry on fatigue life of aircraft structural cylinder part, *Engineering Failure Analysis*, 16 (2009) 1203-1207.

[17] Anish, A. Kumar and A. Chakrabarti, Failure mode analysis of laminated composite sandwich plate, *Engineering Failure Analysis*, 104 (2019) 950-976.

[18] A. Kumar et al., Efficient failure analysis of laminated composites and sandwich cylindrical shells based on higher-order zigzag theory, *Journal of Aerospace Engineering*, 28 (2015) 1-14.

[19] S. Bazazzadeh, M. Zaccariotto and U. Galvanetto, Fatigue degradation strategies to simulate crack propagation using peridynamic based computational methods, *Latin American Journal of Solids and Structures*, 16 (2019) e163.

[20] S. Bazazzadeh, F. Mossaiby and A. Shojaei, An adaptive thermo-mechanical peridynamic model for fracture analysis in ceramics, *Engineering Fracture Mechanics*, 223 (2020) 106708.
[21] B. Averbach and E. Bamberger, Analysis of bearing incidents in aircraft gas turbine mainshaft bearings, *Tribology Transactions*, 34 (1991) 241-247.
[22] N. Ejaz, I. Salam and A. Tauqir, Failure analysis of an aero engine ball bearing, *Journal of Failure Analysis and Prevention*, 6 (2006) 25-31.
[23] G. Jacobs and M. Plogmann, Rolling bearing damages, *Encyclopedia of Lubricants and Lubrication*, Springer (2014) 1600-1618.
[24] T. Yamashita and P. Hayes, Analysis of XPS spectra of Fe2+ and Fe3+ ions in oxide materials, *Applied Surface Science*, 254 (2008) 2441-2449.
[25] J. Gegner, Tribological aspects of rolling bearing failures, *Tribology-Lubricants and Lubrication*, InTech, Rijeka, Croatia (2011).
[26] P. K. Gupta, Current status of and future innovations in rolling bearing modeling, *Tribology Transactions*, 54 (2011) 394-403.
[27] Q. Gao et al., Cause analysis and risk assessment of skidding stripe on aeroengine cylindrical roller bearing, *Mechanical Research & Application*, 32 (2019) 85-88.
[28] F. Xu et al., Microstructure modifications and corrosion behaviors of cr4mo4v steel treated by high current pulsed electron beam, *Materials Chemistry and Physics*, 126 (2011) 904-908.
[29] D. Luo et al., The microstructure of ta alloying layer on m50 steel after surface alloying treatment induced by high current pulsed electron beam, *Vacuum*, 136 (2016) 121-128.
[30] J. Zou et al., Mechanisms of nanostructure and metastable phase formations in the surface melted layers of a hcpeb-treated D2 steel, *Acta Materialia*, 54 (2006) 5409-5419.
[31] Z. Cai et al., Development of a novel cycling impact-sliding wear rig to investigate the complex friction motion, *Friction*, 7 (2019) 32-43.
[32] B. Bhushan, *Principles and Applications of Tribology,* John Wiley and Sons, New Jersey, USA (1999).
[33] H. Zhang et al., Modeling of elastic finite-length space rolling-sliding contact problem, *Tribology International*, 113 (2017) 224-237.
[34] S. Wen and P. Huang, *Tribology Principle*, Tsinghua University Press, Beijing, China (2002).
[35] L Cui and Y. He, A new logarithmic profile model and optimization design of cylindrical roller bearing, *Industrial Lubrication and Tribology*, 67 (2015) 498-508.

Xiangyu Xie received his master degree in Mechanical Engineering in 2017 from Guizhou University, China. Now, he is currently a lab master at Guiyang University, China. His research interest is tribology of bearing and failure analysis.

Jin Xu received his Ph.D. degree from Southwest Jiaotong University in 2003. His current position is the assistant research fellow and tutor of master degree candidates in Guizhou University, China. His research interests include tribology and surface engineering.

Jun Luo received his Ph.D. degree from Southwest Jiaotong University in 2011. His current position is a Professor at Guiyang University, China. His research interests include surface engineering and wear.